JOURNAL OF GEOPHYSICAL RESEARCH, VOL. 97, NO. C1, PAGES 627–638, JANUARY 15, 1992

Primary Production Estimates from Recordings of Solar–Stimulated Fluorescence in the Equatorial Pacific at 150°W

P. M. STEGMANN[1] AND M. R. LEWIS

Department of Oceanography, Dalhousie University, Halifax, Nova Scotia, Canada

C. O. DAVIS

Jet Propulsion Laboratory, California Institute of Technology, Pasadena

J. J. CULLEN

Bigelow Laboratory for Ocean Sciences, West Boothbay Harbor, Maine

Biological, optical, and hydrographical data were collected on the WEC88 cruise along 150°W and during a 6–day time series station on the equator during February/March 1988. This area was characterized by a subsurface chlorophyll maximum (SCM), located at 50–70 m depth at the equator and descending down to 120–125 m at the north and south end of the transect. Highest primary production rates were near–surface and confined to the equatorial region and stations between 7° and 11°N. To determine the relationship between solar–stimulated fluorescence (centered at 683 nm wavelength) and primary production, a production–fluorescence model based on phytoplankton physiology and marine optics is described. Results of model calculations predict that there is a linear relation between production and fluorescence. A comparison between morning and midday measurements of the production–fluorescence relation showed that there was some difference between the two, whereas evening measurements, on the other hand, were distinctly different from the morning/midday ones. This seems to suggest that diurnal variations contribute significantly to variability in the quantum yield of photochemical processes. The ratio of the quantum yield of photosynthesis to the quantum yield of fluorescence (Φ_c/Φ_f), the parameter which will determine how well production can be estimated from optical recordings, ranged between 0.24 and 0.44 molC Ein^{-1} (an Einstein equals a mole of photons) for all stations. The highest value for this ratio occurred at the equatorial stations, indicating that interstation (i.e., latitudinal) variability could have an effect on the production–fluorescence relation. Measured (with ^{14}C incubations) and predicted production compared quite well, although high measured production rates for near–surface samples were underestimated in most cases. Since both production and fluorescence were nonlinear at high irradiance intensities, we recommend in the future that a nonlinear component be incorporated into our model to take this effect into account and thus allow us to refine our estimates of nonlinear data.

1. INTRODUCTION

Understanding the role of the oceans in global biogeochemical cycles is one of the major goals of the Global Ocean Flux Study [*National Academy of Sciences*, 1984]. For this purpose, satellite observations of phytoplankton biomass and productivity provide the only means to obtain synoptic information on the time and space scales of interest. Specifically, remote recordings of the optical properties of the upper ocean allow inferences to be made about the transformation of important elements, especially carbon, within the productive layer. The next generation of Earth–observing platforms will have sensors with the sensitivity and spectral resolution necessary to make these measurements. The key to making use of these measurements is to develop and validate appropriate models relating the measured optical properties with phytoplankton biomass and productivity.

A method which shows substantial promise for the remote estimation of phytoplankton biomass and primary production utilizes the solar–stimulated fluorescence signal emitted by phytoplankton, which is centered at 683–685 nm wavelength [*Neville and Gower*, 1977; *Gower and Borstad*, 1981, 1990; *Kishino et al.*, 1984*a,b*; *Topliss*, 1985; *Topliss and Platt*, 1986; *Kiefer et al.*, 1989; *Chamberlin et al.*, 1990; *Stegmann*, 1987*a,b,c*]. This method has several advantages which make it attractive over other passive methods. First, fluorescence emission is specific for chlorophyll *a* and its derivatives but not for other suspended matter co–occurring with phytoplankton [*Lin et al.*, 1984]. This is particularly significant for measurements in estuarine or coastal regions, where there is usually a high suspended sediment load as well as yellow substances which can mask the signal in the other passive methods [*Højerslev*, 1981]. Second, when measuring changes in ocean color to obtain information on phytoplankton biomass, high chlorophyll concentrations reduce the water–leaving radiance to very low levels in the wavelengths of maximum absorption, making the signal

[1]Now at Graduate School of Oceanography, University of Rhode Island, Narragansett.

Paper number 91JC02014.
0148–0227/92/91JC–02014$05.00

difficult to measure from space [*Sathyendranath and Morel*, 1983]. The opposite is true when recording solar–stimulated fluorescence; the signal increases with increasing chlorophyll concentration. And finally, apart from a strong absorption band at 687 nm [*Gower and Borstad*, 1990], atmospheric correction algorithms used to extract the signal from the background noise when recording from space are less complicated than those required for the ocean color method [*Schanda*, 1986].

The major logistical limitation with solar–stimulated fluorescence is that water has a very high absorption coefficient at 683–685 nm, and consequently, the water–leaving radiance is low, particularly in low–chlorophyll waters. Nevertheless, the signal has been measured with an airborne fluorescence line imager [*Gower and Borstad*, 1981, 1990], and future satellite instruments such as MODIS will have channels for measuring solar–stimulated fluorescence [*Esaias*, 1986]. Also, the physiological basis of this type of fluorescence is not yet completely understood [e.g., *Kolber et al.*, 1990].

Recordings of solar–stimulated fluorescence have primarily been used to estimate phytoplankton biomass in the upper ocean [e.g., *Neville and Gower*, 1977]. However, fluorescence emission is linked to the physiological processes governing photosynthesis, and several attempts have been made to estimate the rate of phytoplankton production from the fluorescence signal [*Topliss and Platt*, 1986; *Kiefer et al.*, 1989; *Chamberlin et al.*, 1990].

Here, we assess the use of the solar–stimulated fluorescence technique to predict the rate of phytoplankton production in the central tropical Pacific Ocean. The characteristic feature of this area is the large–scale divergence due to the Coriolis force and to the trade winds to the north and south, thereby resulting in the large–scale circulation system and water transport described by *Wyrtki* [1981]. This results in equatorial upwelling of nutrient–rich deep water to the surface layer and elevated concentrations of chlorophyll [*Barber*, this issue]. Increased autotrophic standing stock is evident in ocean color estimates of phytoplankton biomass (chlorophyll) from Coastal Zone Color Scanner images [G. Feldman, personal communication, 1990]. Recent approximations of new production in the equatorial Pacific suggest that this area contributes between 18% and 56% of global new production and therefore contributes to the flux of particulate organic carbon out of the oceans' euphotic zone [*Chavez and Barber*, 1987]. However, these estimates are based on a small data set, constrained by the limited spatial coverage of research vessels. Clearly, the equatorial Pacific is an important region in the global carbon cycle, and the processes which regulate new production need to be understood. The scale of this vast system, and the limitations of shipboard sampling, provide a compelling case for remote prediction of phytoplankton production on synoptic scales.

2. Basic Concepts of Production–Fluorescence Model

Fluorescence

Consider the emission of fluorescence by phytoplankton cells in the ocean,

$$F_f(z) = B \int_{\lambda=400}^{\lambda=700} \Phi_f(z, \lambda) \cdot {}^*a_c(z, \lambda) \cdot E_d(z, \lambda)\, d\lambda, \quad (1)$$

where the emitted fluorescence F_f at depth z (Ein m^{-3} s^{-1}) is represented by a Gaussian emission line, assumed to have a half–bandwidth of 25 nm and centered at 683 nm wavelength [*Gordon*, 1979]. The absorption of downwelled irradiance (E_d (z, λ); moles m^{-2} s^{-1}) by phytoplankton pigments (B; mgChl m^{-3}) is governed by the specific absorption coefficient for chlorophyll (${}^*a_c$ (z, λ); m^2 $(mgChl)^{-1}$). The efficiency with which fluorescence is emitted relative to the irradiance absorbed is controlled by the dimensionless quantum yield of fluorescence, Φ_f. All the parameters except B are, in principle, wavelength–dependent over the visible spectrum, 400–700 nm. We assume uniform biomass distribution with depth. (Note that Table 1 is a list of symbols used in the text.)

Recordings of solar–stimulated fluorescence are made by a radiometer which generally measures upwelled radiance centered at 683 nm (L_u683; Ein m^{-2} s^{-1} nm^{-1} sr^{-1}). The measured upwelled radiance at depth l is related to the emitted fluorescence, F_f , by

$$L_u683(l) = C \int_{z=l}^{\infty} F_f \cdot e^{(-K_f(z-l))}\, dz, \quad (2)$$

where contributions from fluorescing cells at depths below the sensor (i.e., over the distance interval z–l) are attenuated by an exponential function weighted by the total diffuse

TABLE 1. List of Symbols Used in Text

Symbol	Definition
F_f	Solar–stimulated fluorescence, Ein m^{-3} s^{-1}
B	Chlorophyll–a concentration, mg m^{-3}
Φ_f	Quantum yield of fluorescence, Ein emitted/Ein absorbed
${}^*a_c$	Specific absorption coefficient for chlorophyll, m^2 $(mgChl)^{-1}$
E_d	Downwelled irradiance, moles m^{-2} s^{-1}
L_u683	Upwelled radiance at 683 nm, Ein m^{-2} s^{-1} nm^{-1} sr^{-1}
E_d683	Downwelled irradiance at 683 nm, Ein m^{-2} s^{-1} nm^{-1}
F_r	Integral fluorescence, Ein m^{-2} s^{-1}
F_c	Instantaneous photosynthetic rate, molC m^{-3} s^{-1}
Φ_c	Quantum yield of photosynthesis, mol C fixed/Ein absorbed
K_f	Total diffuse attenuation coefficient at 683 nm, m^{-1}
K_t	Total diffuse attenuation coefficient over PAR, m^{-1}

attenuation coefficient for fluorescence at 683 nm radiance, K_f (m^{-1}). C is a constant and is equal to the product of the geometric correction ($4\ \pi sr^{-1}$) times the correction for the fluorescence bandwidth ($25\ nm^{-1}$) [*Gordon*, 1979]; its value is 0.0032. We have set the upper limit of integration to infinity, since solar-stimulated fluorescence declines with depth and then becomes insignificant. For radiance measurements made near the seasurface, there is also a significant contribution by sunlight backscattered into the field of view of the sensor by seawater itself. In order to obtain only that part of the radiance signal due to phytoplankton fluorescence, a correction must be applied to account for this additional radiance contribution. This was done by subtracting the correction equation below from the $L_u 683(l)$ signal as follows:

$$L_u 683c(l) = L_u 683(l) - (E_d 683(l - 0.38) \cdot 0.00026 \cdot e^{(-K_f \cdot 0.38)}), \quad (3)$$

where $E_d 683(l-0.38)$ is the downwelled irradiance at 683 nm, measured at the top of the spectroradiometer, and $L_u 683c$ is the corrected fluorescence signal. The value 0.00026 is the reflectance value for clear seawater (i.e., water containing no attenuating dissolved/particulate substances) at 683 nm [*Chamberlin et al.*, 1990], and 0.38 m is the length of the spectroradiometer between the $E_d 683$ and $L_u 683$ sensors. The conversion from the corrected fluorescence radiance signal to a fluorescence irradiance signal, F_r (Ein $m^{-2}\ s^{-1}$) is

$$F_r(l) = L_u 683c(l) / C, \quad (4)$$

where C is the conversion constant described above.

Photosynthesis

The rate of photosynthetic carbon fixation is assumed to be a function of the absorbed irradiance as in equation (1), so that

$$F_c(z) = B \int_{\lambda=400}^{\lambda=700} \Phi_c(z, \lambda) \cdot {}^*a_c(z, \lambda) \cdot E_d(z, \lambda)\, d\lambda, \quad (5)$$

where all the terms are the same as above, except that $F_c(z)$ is the instantaneous rate of photosynthesis (molC $m^{-3}\ s^{-1}$) and Φ_c is the quantum yield of photosynthesis (molC Ein^{-1}). To compare this with measured fluorescence, a depth-integrated measure, we also integrate $F_c(z)$ from the depth of the sensor to infinity, assuming B is constant.

Fluorescence and Photosynthesis

There is a connection between the rate of photosynthesis and fluorescence, since both depend on the absorption of incident irradiance by the photochemical apparatus. There are, however, other processes which are associated with light absorption, and these result in the production of heat. Here we model heat production as a dimensionless quantum yield. When one transforms the units for fluorescence, photosynthesis, and heat production into the same units as absorbed energy, then conservation of energy requires that the sum of the quantum yields equals one. Without a separate estimate of heat production though, the problem is underspecified. When determining a functional relation between photosynthesis and fluorescence, the key assumption requires that the ratio of the quantum yields of photosynthesis to fluorescence remains relatively invariant. Or alternatively, one can predict the fluctuation of this ratio as a function of other measurable environmental variables, e.g., irradiance [*Chamberlin et al.*, 1990].

Let us examine the simplest case to demonstrate this requirement. We first assume that all parameters except irradiance are independent of depth. Second, we assume that all parameters are wavelength-independent and that the wavelength-dependent irradiance E_d can be replaced by the irradiance integrated over the spectrum of photosynthetic available radiation (PAR; 400–700 nm, Ein $m^{-2}\ s^{-1}$). The recorded radiance from the fluorescence signal after integration of equation (2) is then

$$F_r(l) = B \cdot \Phi_f \cdot {}^*a_c \cdot E_d(PAR) \cdot \frac{1}{K_t + K_f}, \quad (6)$$

where K_t is the total diffuse attenuation coefficient over the PAR spectrum. Applying these same assumptions to integral photosynthesis leads to

$$\int_{z=l}^{\infty} F_c(z)\, dz = B \cdot \Phi_c \cdot {}^*a_c \cdot E_d(PAR) \cdot \frac{1}{K_t}. \quad (7)$$

After rearranging equations (6) and (7) and cancelling out the common terms, prediction of integral photosynthesis from fluorescence recordings is

$$\int_{z=l}^{\infty} F_c(z)\, dz = \frac{\Phi_c}{\Phi_f} \cdot F_r(l) \cdot \frac{K_t + K_f}{K_t}. \quad (8)$$

Except for the ratio of the quantum yields, all terms on the right side are either measured or known á priori. This is a very simple equation; and although it does ignore all nonlinearities in both the photosynthesis–irradiance and fluorescence–irradiance relationships as well as any depth variation of chlorophyll or wavelength-dependence of any of the parameters, it is a good place to start, since the model is easily tested by linear regression of integral photosynthesis on the terms on the right-hand side of equation (8). The regression coefficient is equal to the ratio of the quantum yields, and its variation can then be examined in more detail.

3. Data Collection and Analysis

General

Data were collected at stations located along a transect from 15°N to 15°S (longitude approximately 150°W) during a 4-week cruise of the R/V *Wecoma* in February/March

1988 that included a 6-day timeseries station at the equator. The focus of this paper is on stations between 15°N and the equator and from the equatorial timeseries stations. Vertical profiles of hydrographical, optical, and biological variables were made with a modified Bio-Optical Profiling System (BOPS [*Smith et al.*, 1984]). The physical parameters measured were temperature, salinity, and depth. The BOPS was equipped with an MER-1048 spectroradiometer (Biospherical Instruments) capable of simultaneously measuring upwelling radiance, upwelling irradiance, and downwelling irradiance in 6, 8, and 13 channels, respectively. Furthermore, this instrument package provided simultaneous measurements of *PAR*, chlorophyll fluorescence (SeaTech Fluorometer), and beam transmission (SeaTech Transmissometer). Water samples were collected with a CTD-rosette system.

Primary Production Measurements

Water samples were collected from four depths with hydrocasts, one to three times per day, and taken shortly before or after the optical casts. The exceptions to this are the evening casts, where the incubations were done after sunset. The rate of photosynthesis versus irradiance at each depth was measured by the addition of ^{14}C labelled samples to 24 vials and then incubating them for 1 hour at 24 different light intensities in modified photosynthetrons according to the procedure described by *Lewis and Smith* [1983]. A temperature-regulated flow-through system was used to keep the incubation temperature close to the in situ temperature. Results were described as a P-I curve with three parameters [*Platt et al.*, 1980] and were corrected for P_o, an intercept, which was treated as a dark bottle, so that the production curve went through zero (see *Cullen et al.* [this issue] for a discussion of this procedure and the limitations of the P versus I methodology). This resulted in estimates of the instantaneous rate of photosynthesis normalized to chlorophyll, which in turn was derived from acetone extracts [*Cullen et al.* this issue]. Continuous vertical profiles of chlorophyll-normalized photosynthesis as a function of depth were calculated from measured irradiance (*PAR*) and P-I parameters; values from the four depths from which the incubation samples had been taken were linearly interpolated to obtain a continuous profile. Production as a function of depth (molC m^{-3} s^{-1}) was obtained by multiplying the chlorophyll-normalized photosynthesis just described by the calibrated chlorophyll-fluorescence profiles (see *Cullen et al.* [this issue] for details on this procedure). At most stations, the deepest depth from which water samples were taken for incubations was 60 m. Since solar-stimulated fluorescence could generally be detected down to 80-100 m, integral photosynthesis was simply extended down to the depth where fluorescence went to zero. This extension was made by assuming that the photosynthetic parameters from the deepest sampling depth remained relatively constant below.

Information pertaining to those sites where both optical casts and production incubations were available is summarized in Table 2; these are the stations which will be used in our fluorescence-production model. Figures which contain mean values (Figures 1-4 and 9) were obtained by averaging all stations over time at the particular latitude.

Determination of Attenuation Coefficients

The total diffuse attenuation coefficient at any wavelength is considered to be equal to the sum of the components in the ocean contributing to attenuation at that wavelength [*Smith and Baker*, 1978]. Specifically, these are the water itself, phytoplankton and associated detritus, and any other particulate or dissolved substances in suspension.

It is generally accepted that in open ocean waters the contribution to the total diffuse attenuation coefficient by all substances other than phytoplankton and the water itself can be disregarded [e.g., *Smith and Baker*, 1978; *Morel and Prieur*, 1977]. It has become common practice to approximate the attenuation due to phytoplankton pigments (K_c) and water (K_w) by the specific absorption coefficient due

TABLE 2. Information on the Optical Cast and Production Stations

Ship Station No.	Optical Cast No.	Date	Position	Time (LDT)	
				Optical Cast	Incubation
8	221a	Feb. 21	12° 28.90′ N, 150° 01.90′ W	0830	0800
11	b		12° 28.15′ N, 150° 03.53′ W	1230	1324
22	223a	Feb. 23	9° 59.41′ N, 150° 00.08′ W	0800	0830
25	b		10° 01.98′ N, 150° 04.08′ W	1330	1212
41	226a	Feb. 26	4° 59.36′ N, 149° 59.32′ W	0800	0700
45	b		4° 59.17′ N, 149° 58.43′ W	1430	1312
48	c		4° 57.66′ N, 149° 59.26′ W	1700	1724
64	228b	Feb. 28	2° 00.33′ N, 150° 05.94′ W	1430	1400
66	c		1° 59.27′ N, 150° 05.94′ W	1700	1912
71	229a	Feb. 29	0° 59.97′ N, 150° 00.93′ W	0800	0730
75	b		0° 57.21′ N, 150° 05.61′ W	1300	1330
77	c		0° 58.96′ N, 150° 01.96′ W	1630	1900
87	302a	March 2	0° 00.36′ N, 150° 01.62′ W	0830	0630
100	303a	March 3	0° 00.08′ N, 149° 59.48′ W	0900	0600
104	b		0° 00.24′ N, 150° 00.03′ W	1300	1200
106	d		0° 00.00′ N, 149° 59.94′ W	1600	1800
114	304a	March 4	0° 00.43′ N, 150° 01.14′ W	0800	0630
118	b		0° 00.33′ N, 150° 00.42′ W	1300	1200
127	305a	March 5	0° 00.23′ S, 150° 00.58′ W	0800	0630
131	b		0° 00.07′ S, 149° 59.76′ W	1300	1200
150	307a	March 7	0° 00.28′ N, 150° 01.05′ W	0800	0630

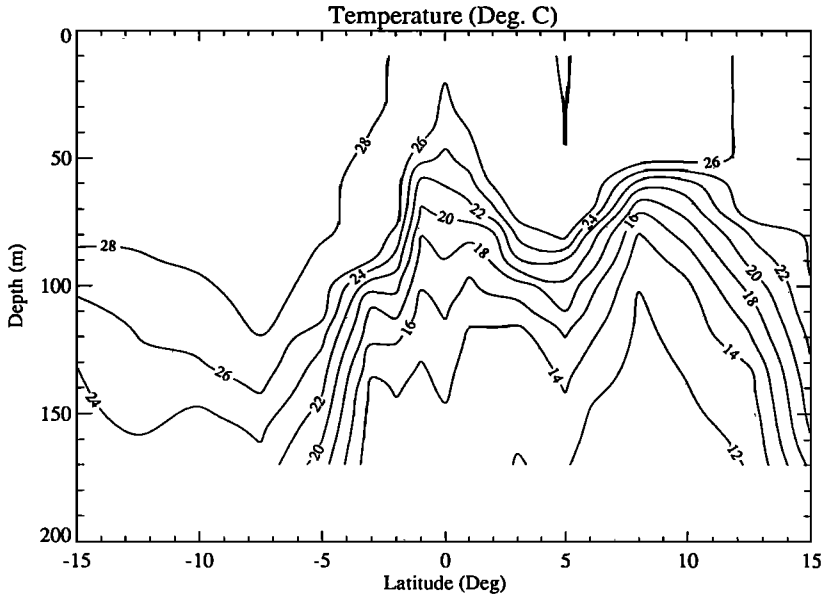

Fig. 1. Temperature (mean; units of $°C$) versus depth for stations along the 15°N to 15°S transect.

to chlorophyll ($^*a_c$) and water (a_w), respectively. Thus at the wavelength of fluorescence emission, the absorption coefficient due to water, $a_w(683)$, is large and is equal to 0.465 m^{-1} [*Morel and Prieur*, 1977; *Smith and Baker*, 1981]. *Kiefer et al.* [1989] found that the specific absorption coefficient for chlorophyll, $^*a_c(683)$, in the western South Pacific gyre was about 0.01 m^2 $(mgChl)^{-1}$. During our cruise the chlorophyll concentration never exceeded 0.5 mg m^{-3} (cf. Figure 2), so that the maximum contribution by $^*a_c(683)$ at this concentration would at most only have been about 1%. We therefore assume that the major attenuating component at 683 nm is water and that $a_w(683)$ is equal to $K_w(683)$ which is equal to K_f .

As *Smith and Baker* [1984] have pointed out, recordings of underwater irradiance are influenced by surface waves and ship roll. The total diffuse attenuation coefficient will consequently also contain these perturbations. To smooth out these fluctuations, we applied a low-pass filter in our calculations of the total diffuse attenuation coefficient over the *PAR* spectrum (K_f). K_f was determined [*Smith and Baker*, 1984] by calculating an average running K_f over 10 depth readings obtained from regressing vertical profiles of log-transformed *PAR* values against depth.

4. Results

Vertical Distributions

The temperature profile from 15°N to 15°S clearly shows the result of equatorial divergence with the doming effect of cooler water (< 28°C) rising to the surface at the equator

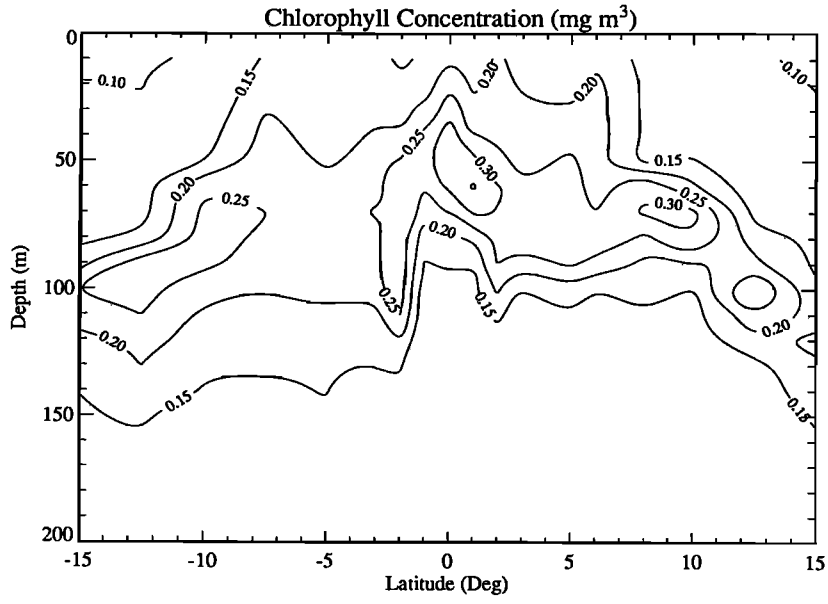

Fig. 2. Chlorophyll *a* concentration (mean; units of mg m^{-3}) versus depth for stations along the 15°N to 15°S transect.

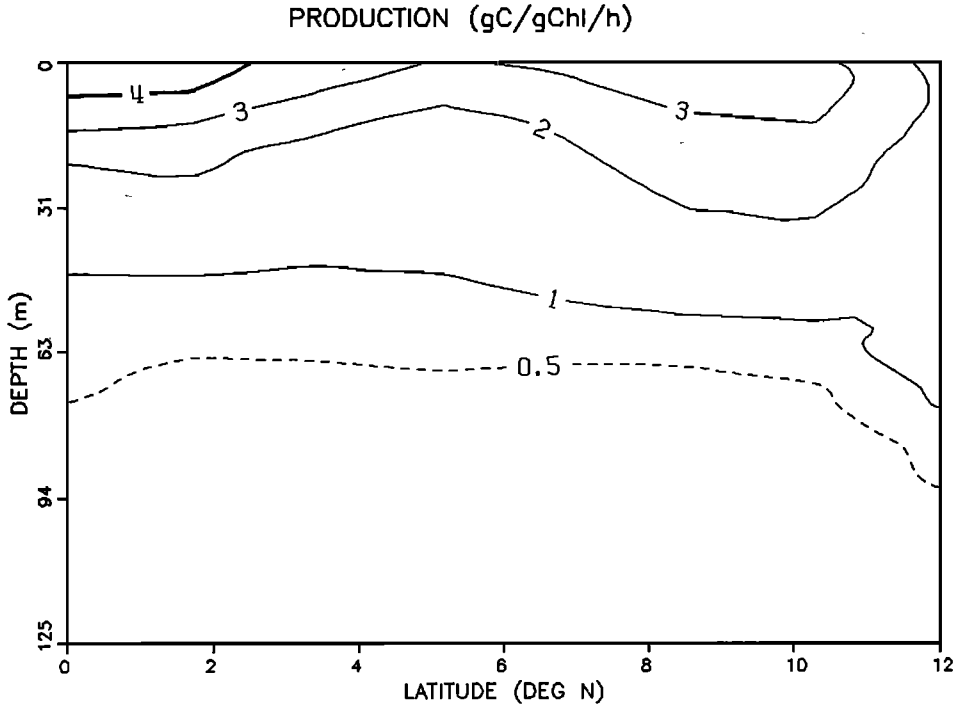

Fig. 3. Production normalized to chlorophyll *a* concentration (mean; units of gC $gChl^{-1}$ h^{-1}) versus depth for stations 12°N to Equator.

(Figure 1). To the north and south of this region, mean surface water temperatures were 27° and 29°C, respectively. A second, although less pronounced, doming feature is seen at about 8°–12°N.

This transect is characterized by a subsurface chlorophyll maximum (SCM) which was located between 40 and 80 m near the equator and extended down to about 120–m depth near 15°N and 15°S (Figure 2). The lens of highest (mean) pigment concentration (> 0.25 mg m^{-3}) occurred at the equator and between 8° and 12°S and was confined to the 40–80 m and 70–110 m depth range, respectively. A second, albeit less pronounced, chlorophyll increase occurred at 6–10°N at about 70–m depth.

The highest primary production rates (mean values > 4 gC $gChl^{-1}$ h^{-1}) were measured in the upper 10 m of the water column and were restricted to stations between

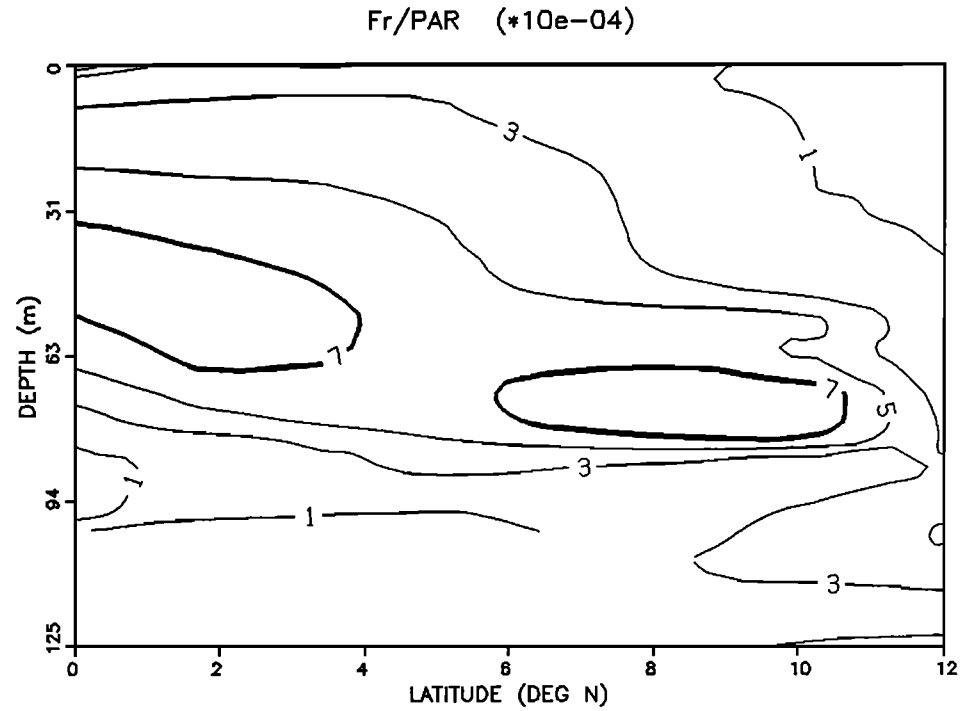

Fig. 4. Ratio of F_r (fluorescence centered at 683 nm wavelength) to PAR (photosynthetic active radiation) (mean; dimensionless) versus depth for stations 12°N to Equator.

3°N and the equator (Figure 3). A second near-surface production maximum occurred between about 11° and 7°N.

The vertical distribution of the ratio F_r/PAR at these same stations should be related to the chlorophyll concentration [*Kiefer et al.*, 1989]. At stations north of the equator the maximum ratio occurred between 70 and 80 m depth, whereas in the equatorial region the maximum was detected between about 35 and 65 m (Figure 4). A comparison of Figures 4 and 2 shows relatively good correspondence between F_r/PAR and phytoplankton biomass.

Fluorescence–Production Relation

To differentiate temporal from spatial (i.e., latitudinal) effects contributing to the variability inherent in our measurements and thus influencing the precision with which we can estimate photosynthesis from recordings of solar-stimulated fluorescence, we have separated the results of our fluorescence–production model calculations into two different parts. For the first part, we wanted to address the question, "Is there a marked temporal effect on the relationship between fluorescence and production?" For this purpose, the results of the linear regression (equation (8)) of integral production on the product of the fluorescence times the ratio of the attenuation coefficients (termed Kratio in Figures 5–7) for the 6-day timeseries station at the equator were considered separate from the rest of the transect stations. These results are shown in Figures 5*a* and 5*b* for the equator morning and midday stations, respectively. The slope of the regression line included in this figure and all subsequent ones of this type is equal to the ratio of the quantum yield of photosynthesis to that of fluorescence, Φ_c/Φ_f (from equation (8); units of molC Ein^{-1}). Values for the slope and the other regression results are shown in Table 3.

The morning stations (Figure 5*a*) show two distinct sets of curves. The reason for this separation is due to a difference in the production rate; the lower set corresponds to lower rates than the upper set. A comparison between the morning and midday stations (Figures 5*a* and 5*b*) at the equator indicated that production and fluorescence were higher at midday than in the morning. The regression analysis yielded a somewhat higher slope for the morning (0.44 molC Ein^{-1}) than for the midday (0.42 molC Ein^{-1}) stations, but a better correlation coefficient for the midday than the morning ones. This first attempt then at assessing the importance of temporal effects (i.e., difference between morning and midday) on the relation between production and fluorescence seems to suggest that, at least at the equator, there is no pronounced difference between these two time periods. Evening stations, on the other hand, are very different and show the lowest slopes of all (cf. Table 3). Although not shown here, this also holds true for the one equator evening station (cf. Table 2), where the slope was 0.23 molC Ein−1. Taken over a whole day then, diel effects clearly are important factors that contribute to variations in the quantum yield.

The second question we wanted to examine with our model calculations was if spatial (latitudinal) differences contributed significantly to the variability in the fluorescence–production relation. To resolve this query, we looked at all stations from 12°N to the equator (listed in Table 2), taking care to group them into morning, midday, and evening stations (Figures 6*a*–6*c*). A first comparison between these three time groups indicated that production and fluorescence were highest at the midday stations and lowest at the evening ones. Furthermore, the quantum yield ratio (= slope) was highest for the morning and lowest for the evening stations (cf. Table 3). As expected, the varying conditions at each individual station resulted in a lower correlation coefficient when all stations were combined than if the equator stations were considered alone. It is interesting to note that, with one exception, the quantum yield ratio was generally higher for the equatorial stations than for the other stations along the transect. Our results thus seem to suggest that (1) interstation variability does have some effect on the production–fluorescence relation and (2) the variation in the quantum yield ratio depended on the time of day the measurements were made (i.e., morning/midday or evening).

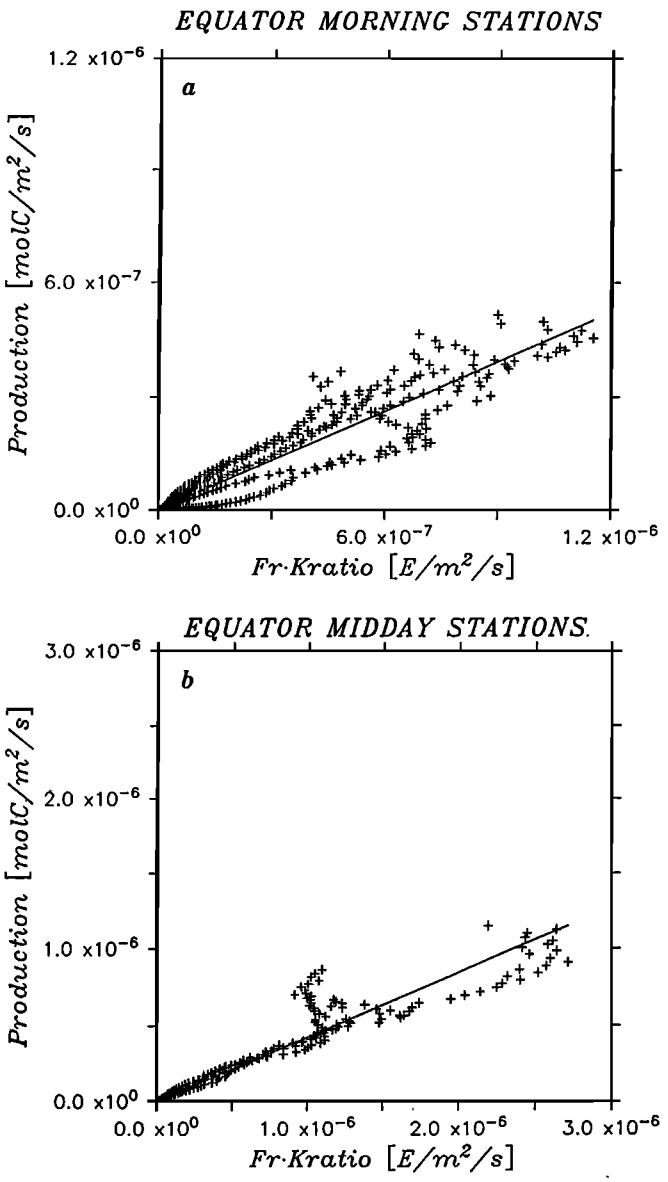

Fig. 5. F_r· Kratio versus integral production for the equatorial stations. (*a*) Morning; $y = 0.44$, $r = 0.929$, $n = 353$, and (*b*) midday; $y = 0.42$, $r = 0.943$, $n = 235$. Obtained by solving equation (8).

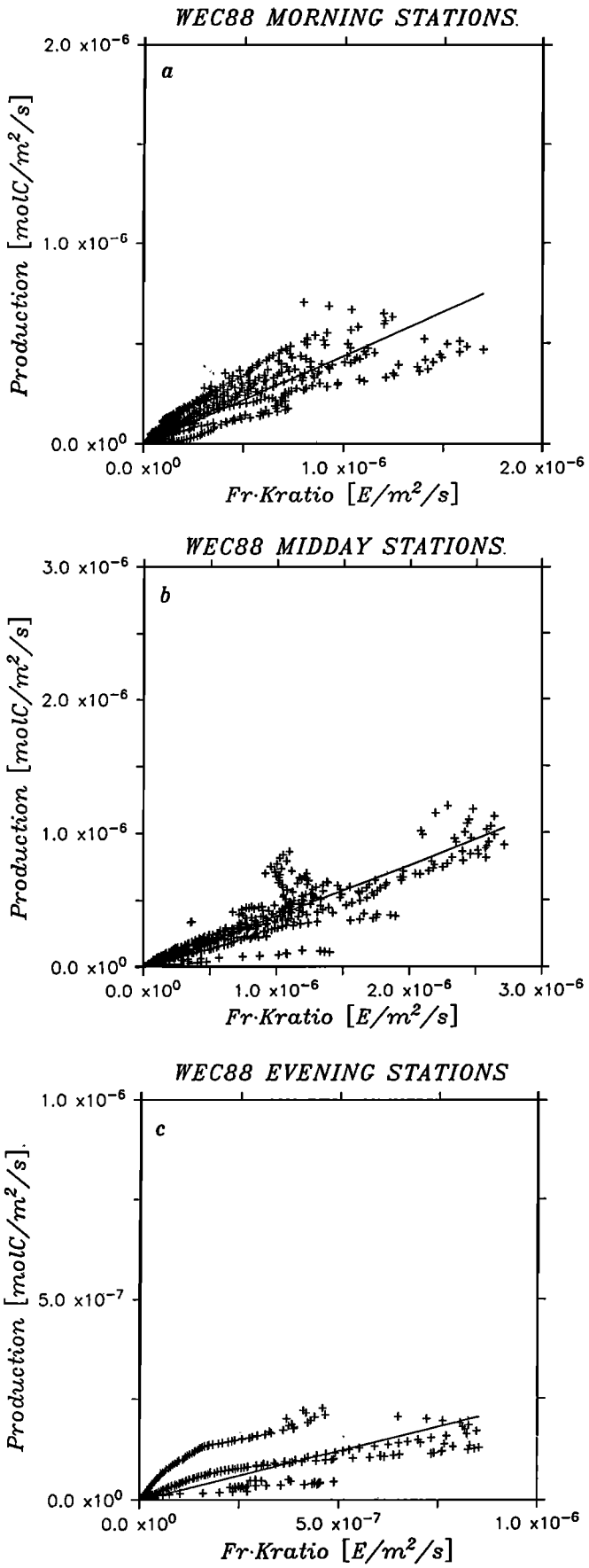

Fig. 6. F_r· Kratio versus integral production for all WEC88 stations. (*a*) Morning; $y = 0.44$, $r = 0.869$, $n = 695$, (*b*) midday; $y = 0.38$, $r = 0.925$, $n = 680$, and (*c*) evening; $y = 0.24$, $r = 0.606$, $n = 270$. Obtained by solving equation 8.

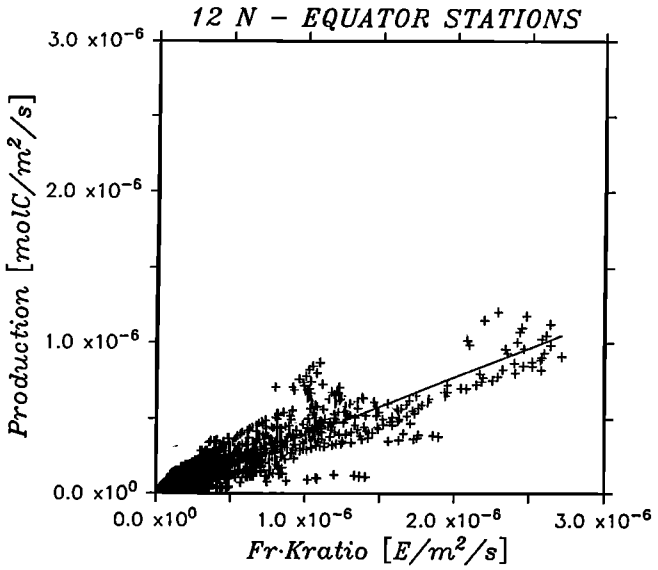

Fig. 7. F_r· Kratio versus integral production for all WEC88 stations; $y = 0.39$, $r = 0.907$, $n = 1645$. Obtained by solving equation (8).

In order to get at least an approximate idea of the relation between production and fluorescence for all stations from 12°N to the equator, irrespective of time of day, all fluorescence and production data were combined and regressed against one another; the result is shown in Figure 7 and Table 3. Despite the fact that these stations covered a large geographical area and the measurements occurred at different times of day, there was still a relatively good fit (correlation coefficient of 0.907) and the ratio of the quantum yields was equal to 0.39 molC Ein^{-1} .

Prediction of Photosynthesis

We now examine in hindcast to what extent our production–fluorescence model tracks the real world. In Figure 8 we have plotted the measured production versus the predicted production (using the the regression equation obtained in Figure 7) for all stations from 12°N to the equator (cf. also Table 3). The line in the figure is a perfect fit and is included only for reference purposes. In general, there is a relatively good correspondence between measured and predicted production, albeit with considerable scatter. For example, at very high rates, production is often underestimated by the model. Clearly, at these near–surface depths, production cannot be predicted satisfactorily with

TABLE 3. Results of Linear Regression Analysis of Fluorescence–Production Model (Equation (8))

	n	Slope	r
Equator stations			
Morning	353	0.44	0.929
Midday	235	0.42	0.943
All stations			
Morning	695	0.44	0.869
Midday	680	0.38	0.925
Evening	270	0.24	0.606
12° N to Equator	1645	0.39	0.907

Here n is number of depth data points used in regression analysis. Slope has units of molC Ein^{-1}.

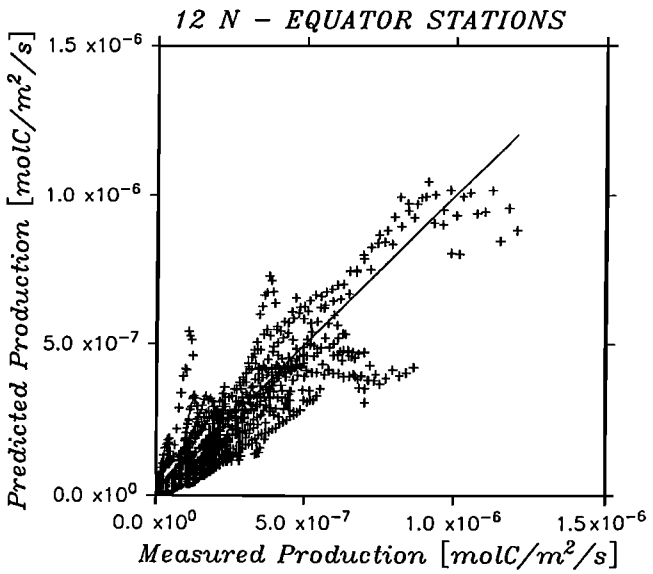

Fig. 8. Measured versus predicted integral production (using results obtained from solving equation (8) for all 12°N to Equator stations. Line represents perfect fit.

our model. Possible explanations for this inconsistency are discussed below.

5. Discussion

Our original intention was to examine the relationship between solar-stimulated fluorescence and phytoplankton production in the central Pacific Ocean from the perspective of using what hopefully were well-correlated variables to estimate photosynthesis in this region. To do this effectively, we examined the variability of the ratio of the quantum yields over a variety of environmental conditions. After all, it is the behavior of this ratio which determines the applicability of remote sensing techniques to estimate photosynthetic rates in the upper ocean. From the following discussion it will become clear that more field work is needed to refine the relationship between fluorescence and photosynthesis, as this will provide the basis for an algorithm to estimate integral production from Earth-observing satellites.

As a first attempt to model the relation between integral production and solar-stimulated fluorescence, we have used simplified principles of phytoplankton physiology and marine optics to develop a simple, linear production-fluorescence model. We have shown that in February/March 1988 there was a clear relation between integral production and solar-stimulated fluorescence in the tropical Pacific. Our results suggest that diel fluctuations (i.e., a comparison between morning/midday with evening measurements) do effect the production-fluorescence relation. Spatial (i.e., latitudinal) differences, which are possibly caused by such factors as photoadaptation, light and nutrient utilization, or species specific variations could also affect the quantum yield ratio. Unfortunately, much of the variation is still unexplained, and more detailed research is needed to understand and interpret the observed variations. Nonetheless, it seems plausible that the variations we observed in the Pacific are strongly influenced by our assuming biomass is constant with depth and also by the selection of the reflectance value used for the backscatter correction (cf. equation (3)).

With the exception of high production levels, which often exceeded the estimate, measured and predicted integral production compared quite well (Figure 8). It seems that when the highest measured production occurs near-surface, the linear relationship between production and fluorescence no longer holds. This can be seen quite clearly when one looks at plots of production profiles (normalized to biomass) as a function of *PAR* profiles (Figure 9*a*): after an initial linear increase at low light intensity, photosynthetic rate attains a maximum value and then begins to leveloff to a relatively constant production rate with little response to further increases in irradiance. The initial slopes of the morning and midday stations are very similar. However, the morning stations begin to leveloff at a lower production rate than the midday ones. The evening stations, on the other hand, have a very different slope as well as lower irradiance values at which they attain their production maximum. A plot of fluorescence (normalized to biomass) as a function of *PAR* profiles (Figure 9*b*) also shows the same general pattern as for the production versus *PAR* profiles (cf. Figure 9*a*). There are, however, two clear differences between the production and the fluorescence plots. First, the initial slope for all three fluorescence versus *PAR* curves are almost

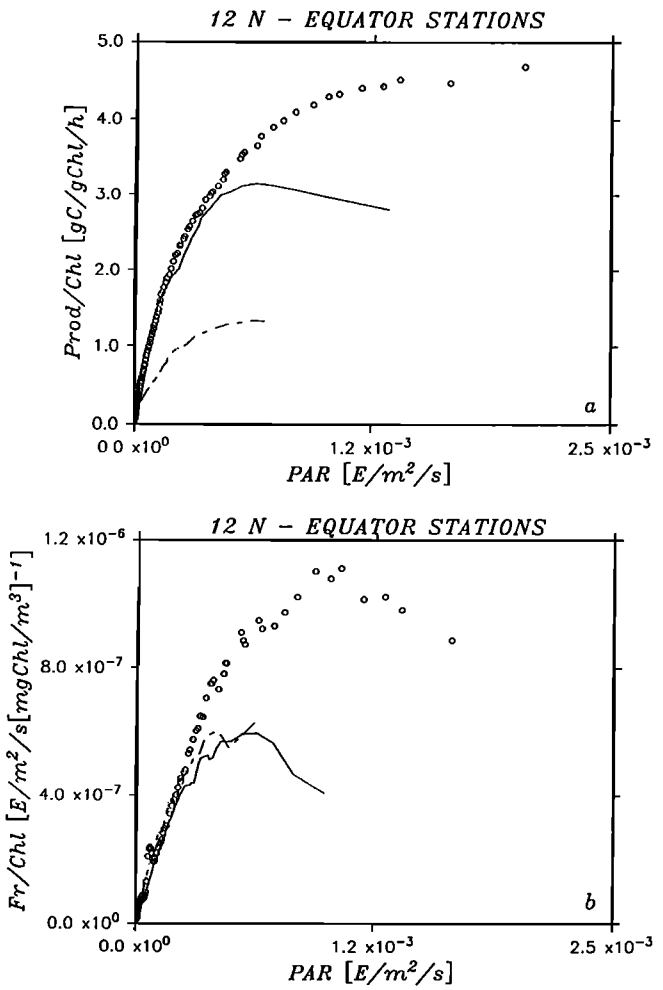

Fig. 9. (*a*) Production normalized to chlorophyll *a* concentration (mean; units of gC m^{-3} h^{-1} (gChl m^{-3})$^{-1}$) and (*b*) F_r normalized to chlorophyll *a* (mean; units of Ein m^{-2} s^{-1} (mgChl m^{-3})$^{-1}$) versus PAR (mean; units of Ein m^{-2} s^{-1}) for all morning (dashed curve), midday (circles), and evening (solid line) stations from 12°N to Equator.

identical. And second, the morning and evening stations leveloff at about the same production rate and irradiance intensity. Thus, in the near–surface region, both production and fluorescence are definitely nonlinear at high irradiance levels. A significant improvement in our linear production–fluorescence model would involve expanding our predictive equation (equation (8)) to account for these nonlinear effects. For the photosynthesis component of our model, equation (4) could be substituted by the relation advanced by *Webb et al.* [1974]:

$$F_c(z) = P_m \cdot (1 - e^{(-{}^*a_c \cdot \Phi_c \cdot E_d(l)/P_m)}), \qquad (9)$$

where P_m is the maximum photosynthetic rate. Integral production [*Lewis et al.*, 1985] would then equal

$$\int_{z=l}^{\infty} F_c(z)\,dz = \frac{-P_m}{K_t} \sum_{n=1}^{\infty} \frac{(-E_d(l) \cdot {}^*a_c \cdot \Phi_c/P_m)^n}{n \cdot n!}. \qquad (10)$$

Since the fluorescence–irradiance relationship looks the same as the production–irradiance relation, a similar equation could easily be developed for the fluorescence component of the model (equation (1)). Incorporation of a nonlinear component and recognizing that the biomass–depth profile is not uniform (as was assumed in the present model) would then hopefully better the precision with which we can predict near–surface photosynthesis. For purposes of future remote sensing from satellites and aircraft, the near–surface zone is the prime determinant for the signal their optical sensors receive.

An interesting result of our model calculations concerned the equator stations (where interstation differences are less evident), where the quantum yield ratio in the morning and at midday were similar. Since we had no independent measure of the specific absorption coefficient for chlorophyll, ${}^*a_c$, we could not determine Φ_c or Φ_f separately and thus know if the similarity in the two quantum yield ratios were due to changes in Φ_c or Φ_f or both. Although the variability has not been sorted out, the ratio of the quantum yields varied by about a factor 2 over the range 0.24–0.44 molC Ein^{-1} (cf. Table 3). This is quite a bit lower than the value obtained by *Chamberlin et al.* [1990] from the western South Pacific gyre but well within the tenfold variations in the quantum yield of photosynthesis determined by *Tyler* [1975], *Priscu* [1984], and *Kishino et al.* [1985]. In fact, the theoretical maximum quantum yield of photosynthesis, assumed to equal 0.125 molC Ein^{-1} and treated as a constant in most studies, can be lowered by as much as a factor of 3 due to nutrient or other physiological–based stress [*Welschmeyer and Lorenzen*, 1981; *Cleveland and Perry*, 1987; *Peterson et al.*, 1988]. The range in the fluorescence quantum yield is still subject to research, but it is not assumed to be a constant. On this basis then, our low quantum yield ratio could be explained by light stress and/or the physiological state of the phytoplankton population. In fact, it has not been completely resolved why the equatorial upwelling region of the Pacific at 150°W did not have a larger phytoplankton biomass in 1988 [*Barber*, this issue]. It seems possible that there is a link between the low phytoplankton biomass and the low quantum yield ratio. Further research is clearly needed to resolve these questions.

How well then does our model compare with other predictive production models based on recordings of solar–stimulated fluorescence? *Chamberlin et al.* [1990] have proposed an empirical formulation relating primary production and solar– stimulated fluorescence. Their equation (16) states that

$$F_c(t,z) = \left(\frac{\Phi_c}{\Phi_f}\right)_{max} \cdot \frac{Kcf \cdot F_f(t,z)}{(Kcf + E_o(PAR,t,z))}, \qquad (11)$$

where F_c and F_f are, respectively, the photosynthetic (molC m^{-3} s^{-1}) and fluorescence (Ein m^{-3} s^{-1}) rates at a given depth z, $(\Phi_c/\Phi_f)_{max}$ is the maximum value of the quantum yield ratio; this empirical constant is equal to 2.3 carbon atoms $photon^{-1}$. Kcf is another empirical constant and is equal to the irradiance when $(\Phi_c/\Phi_f)_{max}$ is half its maximum value; it is equal to 133 μEinm^{-2} s^{-1}. For derivations of these two constants we refer the reader to *Chamberlin et al.* [1990]. $E_o(PAR)$ is the same as our $E_d(PAR)$. In order therefore to predict production with the Chamberlin et al. model, we used their empirical constants and introduced our measured values of $E_o(PAR)$ and F_f into the above equation. The result is a comparison between predicted and measured production (F_c) as a function of fluorescence (F_f) and is depicted in Figure 10. Despite the large scatter in the measured values, predicted production with their equation (16) very clearly overestimates the actual measured rates of primary production. The most probable reason for such an unsatisfactory comparison between predicted (using their model) and measured production is the use of constant empirical values. Further studies on the variability of these factors would be extremely beneficial and might resolve this inconsistency. Obviously, a single equation with one set of constants is not adequate as a predictive tool for other oceanic regions. In fact, there are insufficient data to really know that the same set of constants can be used over an annual cycle at the same location. It should, however, also

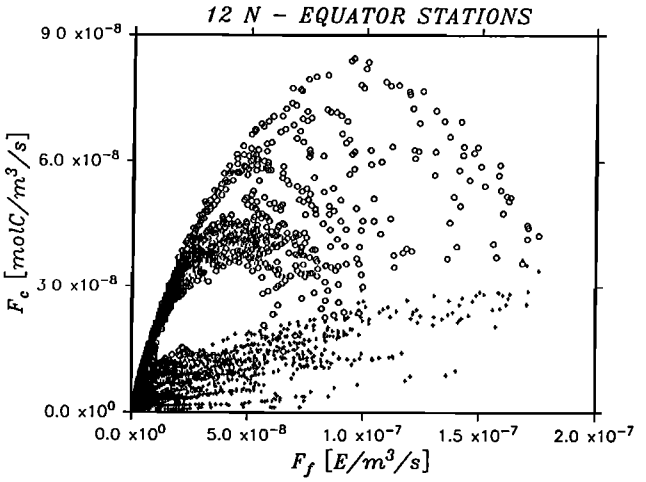

Fig. 10. Production (F_c; molC m^{-3} s^{-1}) versus fluorescence volume emission (F_f; Ein m^{-3} s^{-1}) for all 12°N to Equator stations. Crosses are measured values from this study; circles are estimated production using *Chamberlin et al.'s* [1990] equation (16) for the same fluorescence values. See text for explanation.

be mentioned that our method of measuring production by estimating photosynthesis as a function of irradiance (P–I) underestimates production determined by in situ bottle experiments [*Cullen et al.* this issue].

As noted during this and previous cruises, the tropical Pacific and, in particular, the equatorial divergence zone is an area of enhanced phytoplankton production. However, a consensus on the contribution of new production in this region to global production is still lacking [e.g., *Chavez and Barber*, 1987; *Eppley and Peterson*, 1979; *Eppley and Renger*, this issue]. In fact, we are still trying to understand why this upwelling region with its high nutrient concentration does not in fact support a larger autotrophic standing stock [*Barber*, this issue; *Cullen et al.* this issue]. Questions about grazing or trace metal effects as possible factors limiting biomass accumulation are still being researched. Clearly, field research focussing on these issues is needed. At the same time, however, it becomes very evident that the resolution of these questions necessitates production estimates that are both rapid and synoptic in character. Our production–fluorescence model introduced here is a step toward the possibility of remotely estimating integral primary production optically. However, recordings of solar–stimulated fluorescence coupled with direct production measurements during different seasons and from diverse areas in the tropical Pacific are required to validate the model. Such future conceived field programs would also be required for validation and interpretation of the signals received from ocean–observing satellite sensors such as MODIS, which will record solar–stimulated fluorescence from space.

Acknowledgments. We wish to thank the captain and crew of the R/V *Wecoma* for their able assistance during this cruise. We also thank Dick Barber, who was chief scientist and the guiding light in organizing this cruise. Thanks are also due to Rob Palmer for technical assistance at sea. We gratefully acknowledge comments made by Dale A. Kiefer and Jim Aiken as well as suggestions made by two anonymous reviewers. This research was funded by the following grants: NASA 161–30–33–40 to C.O.D., ONR N00014–87K–0311–01 and NASA NAGW 2072 to J.J.C., NSERC (Canada) Strategic Grant to M.R.L., NSERC (Canada) International Scientific Exchange Award to J.J.C. and M.R.L., and a World University Services of Canada Postdoctoral Fellowship to P.M.S.

REFERENCES

Barber, R.T., Introduction to the WEC88 cruise: An investigation into why the Equator is not greener, *J. Geophys. Res.*, this issue.

Chamberlin, W.S., C.R. Booth, D.A. Kiefer, J.H. Morrow, and R.C. Murphy, Evidence for a simple relationship between natural fluorescence, photosynthesis, and chlorophyll in the sea, *Deep-Sea Res., 37,* 951–973, 1990.

Chavez, F.P., and R.T. Barber, An estimate of new production in the equatorial Pacific, *Deep-Sea Res., 34,* 1229–1243, 1987.

Cleveland, J.S., and M.J. Perry, Quantum yield, relative specific absorbance and fluorescence in nitrogen–limited *Chaetoceros gracilis, Mar. Biol., 94,* 489–497, 1987.

Cullen, J.J., M.R. Lewis, C.O. Davis, and R.T. Barber, Photosynthetic characteristics and estimated growth rates indicate grazing is the proximate control of primary production in the equatorial Pacific, *J. Geophys. Res.*, this issue.

Eppley, R.W., and B.J. Peterson, Particulate organic matter flux and planktonic new production in the deep ocean, *Nature, 282,* 677–680, 1979.

Eppley, R.W., and E.H. Renger, Nitrate utilization by plankton in the equatorial Pacific, March 1988 along 150°W, *J. Geophys. Res.*, this issue.

Esaias, W., MODIS–Moderate–resolution imaging spectrometer, Instrument Panel Report, 59 pp., NASA, Washington, D.C., 1986.

Gordon, H.R., Diffuse reflectance of the ocean: The theory of its augmentation by chlorophyll *a* fluorescence at 685 nm, *Appl. Opt., 18,* 1161–1166, 1979.

Gower, J.F.R., and G. Borstad, Use of the in vivo fluorescence line at 685 nm for remote sensing surveys of surface chlorophyll *a*, in *Oceanography From Space,* edited by J.F.R. Gower, pp. 329–338, Plenum, New York, 1981.

Gower, J.F.R., and G. Borstad, Mapping of phytoplankton by solar–stimulated fluorescence using an imaging spectrometer, *Int. J. Remote Sens., 11,* 313–320, 1990.

Højerslev, N.K., Assessment of some suggested algorithms on sea color and surface chlorophyll, in *Oceanography From Space,* edited by J.F.R. Gower, pp. 347–353, Plenum, New York, 1981.

Kiefer, D.A., W.S. Chamberlin, and C.R. Booth, Natural fluorescence of chlorophyll *a*: relationship to photosynthesis and chlorophyll concentration in the western South Pacific gyre, *Limnol. Oceanogr., 34,* 868–881, 1989.

Kishino, M., S. Sugihara, and N. Okami, Influence of fluorescence of chlorophyll *a* on underwater upward irradiance spectra, *La Mer, 22,* 224–232, 1984*a*.

Kishino, M., S. Sugihara, and N. Okami, Estimation of quantum yield of chlorophyll *a* fluorescence from the upward irradiance spectrum in the sea, *La Mer, 22,* 233–240, 1984*b*.

Kishino, M., N. Okami, M. Takahashi, and S. Ichimura, Light utilization efficiency and quantum yield of phytoplankton in a thermally stratified sea, *Limnol. Oceanogr., 31,* 557–566, 1985.

Kolber, Z., K.D. Wyman, and P.G. Falkowski, Natural variation in the photosynthetic energy conversion efficiency: A field study in the Gulf of Maine, *Limnol. Oceanogr., 35,* 72–79, 1990.

Lewis, M.R., and J.C. Smith, A small–volume, short–incubation time method for the measurement of photosynthesis as a function of incident irradiance, *Mar. Ecol. Prog. Ser., 13,* 99–102 1983.

Lewis, M.R., R.E. Warnock, and T. Platt, Absorption and photosynthetic action spectra for natural phytoplankton populations: Implications for production in the open ocean, *Limnol. Oceanogr., 30,* 794–806, 1985.

Lin, S., G.A. Borstad, and J.F.R. Gower, Remote sensing of chlorophyll in the red spectral region, in *Remote Sensing of Shelf Sea Hydrodynamics,* edited by J.C.J. Nihoul, pp. 317–386, Elsevier, New York, 1984.

Morel, A., and L. Prieur, Analysis of variations in ocean color, *Limnol. Oceanogr., 22,* 709–722, 1977.

National Academy Of Sciences, *Global Ocean Flux Study: Proceedings of a Workshop,* 360 pp., National Academy Press, Washington, D.C., 1984.

Neville, R.A., and J.F.R. Gower, Passive remote sensing of phytoplankton via chlorophyll *a* fluorescence, *J. Geophys. Res., 82,* 3487–3493, 1977.

Peterson, R.B., M.N. Sivak, and D.A. Walker, Relationship between steady–state fluorescence yield and photosynthetic efficiency in spinach leaf tissue, *Plant Physiol., 88,* 158–163, 1988.

Platt, T., C.L. Gallegos, and W.G. Harrison, Photoinhibition of photosynthesis in natural assemblages of marine phytoplankton, *J. Mar. Res., 38,* 687–701, 1980.

Priscu, J.C., In situ quantum yield of phytoplankton in a subalpine lake, *J. Plankton Res., 6,* 531–542, 1984.

Sathyendranath, S., and A. Morel, Light emerging from the sea–interpretation and uses in remote sensing, in *Remote Sensing Applications in Marine Science and Technology,* edited by A.P. Cracknell, pp. 323–357, D. Reidel, Hingham, Mass., 1983.

Schanda, E., *Physical Fundamentals of Remote Sensing,* 187 pp., Springer–Verlag, Berlin, 1986.

Smith, R.C., and K.S. Baker, Optical classification of natural waters, *Limnol. Oceanogr., 23,* 260–267, 1978.

Smith, R.C., and K.S. Baker, Optical properties of the clearest natural waters (200–800 nm), *Appl. Opt., 20,* 177–184, 1981.

Smith, R.C., and K.S. Baker, The analysis of ocean optical data, *Proc. SPIE Int. Soc. Opt. Eng.*, 489, 119–126, 1984.

Smith, R.C., C.R. Booth, and J.L. Star, Oceanographic biooptical profiling system, *Appl. Opt., 23,* 2791–2797, 1984.

Stegmann, P.M., Untersuchungen zur Variabilität der sonnenlichtangeregten Fluoreszenz von Phytoplankton in der Ostsee im Hinblick auf Fernerkundung, *Rep. 169,* 157+43 pp., Institute for Marine Research, University of Kiel, Germany, 1987*a*.

Stegmann, P.M., Sunlight–stimulated fluorescence and phytoplankton development in the Western Baltic Sea, paper presented at IUGG meeting, Vancouver, 1987*b*.

Stegmann, P.M., Solar–stimulated fluorescence and its implications for remote sensing (abstract), *Eos Trans. AGU, 68,* 1694, 1987*c*.

Topliss, B.J., Optical measurements in the Sargasso Sea: Solar–stimulated chlorophyll fluorescence, *Oceanol. Acta, 8,* 263–270, 1985.

Topliss, B.J., and T. Platt, Passive fluorescence and photosynthesis in the ocean: Implications for remote sensing, *Deep-Sea Res., 33,* 849–864, 1986.

Tyler, J.E., The in situ quantum efficiency of natural phytoplankton populations, *Limnol. Oceanogr., 20,* 976–980, 1975.

Webb, W.L., M. Newton, and D. Starr, Carbon dioxide exchange of *Alnus rubra*: A mathematical model, *Oecologia, 17,* 281–291, 1974.

Welschmeyer, N.A., and C.J. Lorenzen, Chlorophyll–specific photosynthesis and quantum efficiency at subsaturating light intensities, *J. Phycol., 17,* 283–293, 1981.

Wyrtki, K., An estimate of equatorial upwelling in the Pacific, *J. Phys. Oceanogr., 11,* 1205–1214, 1981.

J.J. Cullen, Bigelow Laboratory for Ocean Sciences, West Boothbay Harbor, ME 04575.

C.O. Davis, Jet Propulsion Laboratory, California Institute of Technology, Pasadena, CA 91109.

M.R. Lewis, Department of Oceanography, Dalhousie University, Halifax, Nova Scotia, B3H 4J1, Canada.

P.M. Stegmann, Graduate School of Oceanography, University of Rhode Island, Narragansett, RI 02882.

(Received June 18, 1990;
accepted July 24, 1991.)